

A. Eberle, W. Staudacher, A. Zech
Messerschmitt-Bölkow-Blohm GmbH
München-Ottobrunn, W-Germany

ABSTRACT

This paper gives a summary of experimental/theoretical investigations

- o Effect of wing planform variations
 - hybrid wings (strakes)
 - short-coupled canards
 - wing tip modifications
- o Invention and optimisation of maneuver devices including a "variable camber"-wing; use of
 - leading edge slats
 - trailing edge single-slotted flaps
- o Development of a 2-D design method for supercritical profiles and experimental proof
- o Application of supercritical aerofoils on wing planforms as mentioned above.

A systematic variation of the diverse modifications allows to analyse their separated and combined effects.

Selected results demonstrate their efficiency for the design of a fighter-type aircraft maneuvering at transonic speeds.

I. INTRODUCTION

Recent progress in modern aerodynamics is based on two topics:

- o Application of supercritical airfoils
- o Invention of hybrid wing planforms.

Supercritical airfoils

Supercritical airfoils were originally designed for advanced performance and economics of transport-type aircraft. A conventional (subsonic) wing will exhibit deteriorations of performance and flying qualities due to shock-induced separation effects, when the critical Mach-number is exceeded. Supercritical wings will allow to fly well above this speed-boundary. The following improvements are then attributed to this unique feature of the airfoil: increase of cruising speed, range, payload and flying qualities and /or any combination therefrom. This may have consequences for the configuration resulting in a thicker wing (less structure weight, more fuel volume) and/or in a less swept wing (lower weight, better handling and low-speed performance) or in a smaller wing (higher wing loading) or in a wing capable of higher load factors and flight altitude.

Any conceivable compromise is depending on the design specification and thus diffe-

rent for transport- or fighter-type aircraft.

Hybrid wing planforms

The invention of hybrid wing planforms should be seen in regard of the contradictory claims made on a fighter wing. On one side there is a demand of good transonic/supersonic performance and flying qualities, on the other side acceptable low speed characteristics should be provided (subsonic maneuvering, take-off and landing performances). This first called claims are favouring slender, thin and highly swept wings, the last ones do just the opposite.

Hybrid wings or strake-wings came out to be a good compromise in solving this problem. The reasons are summarized below. The strake wing may be considered as a combination of a linear (potential theory) lift producing basic wing (moderately swept with an effective contribution of leading edge suction) with a slender, highly swept inboard leading edge extension. This strake will produce a considerable amount of nonlinear lift at higher angles of attack due to its stable separated spiral vortex system fed from the sharp leading edge. Hence both wing-types exhibit different flow characteristics, each of them well known for itself. Proper combination of the two planforms allow to withdraw specific benefits due to a certain amount of positive interference between the different types of flow. This holds true when there is a "work-sharing" of production of lift (and consequently sharing of "costs" in terms of drag) favouring the positive interference of the basic wing on the strake for low angles of attack, whilst for high angles of attack the stable strake vortex flow should induce favourably on the basic wing.

Hence the following improvements can be expected due to the additional strake:

subsonic/transonic:

- higher maximum lift
- reduced lift dependent drag for high angle of attack
- higher usable lift limits (buffet lift and reduced buffet intensity)
- higher drag divergence M-number

supersonic:

- reduced wave drag
- reduced trim drag

*This research was supported by the German Ministry of Defence

The purpose of this paper is to give selected results based on a fighter-type pilot model and achieved by:

- o invention of hybrid wings
- o application of supercritical aerofoils
- o addition of maneuver devices (slats and flaps)
- o combinations of these means

II. SCOPE OF PROGRAM

The experimental 3-d approach is sketched in Fig. 1.

Part of this research was integrated into the program of a working group "Wings with controlled separation", which was instituted by the German Ministry of Defence (cooperation of DFVLR, MBB and VFW-Fokker). All wind tunnel tests were carried out in close collaboration with the DFVLR-AVA Göttingen in the 3 x 3 m low speed and 1 x 1 m Transonic Tunnel of AVA-Göttingen. The pilot models consisted (figure 1) of different basic wings and their modifications, combined with constant shapes of fuselage and tail surfaces.

Basic wing ① was used primarily to find the effects of strake planforms preselected in water tunnel tests, and, for optimization of maneuver devices including their application for a "variable camber" wing (deflection as a function of a.o.a. and M-number).

Finally the efficiency of short coupled canards was compared with that of the strakes (wetted area was kept constant for both devices).

Basic wing ② could be modified by two different wing tips, a straight one and rounded Bagley-type one. Clipping off the tips gave an additional $AR = 3.45$ wing. Further variations result from addition of strake ⑩ (analogue of strake ①, see basic wing ①) and a further strake planform ⑪ with a curved leading edge giving a smooth interfairing strake/basic wing. In addition a set of maneuver devices was provided. The system was scaled from basic wing ① and adjusted at the same optimized positions.

Basic wing ③ differs from wing ② only by the application of a supercritical airfoil. The theoretical/experimental input for derivation of this section is not shown in fig. 1 but will be described later.

All other modifications (strakes, wing tips, maneuver flaps) are in strict analogy to wing ① and ②, thus giving a direct comparison between their respective effects. In a last step an attempt was made to area-rule the original wing body configuration ③ by adding volume to the strake, wing body intersection and canopy region.

III. RESULTS

The subsequent presentation of results concentrates on longitudinal performances and is directly in line with the approach sketched in fig. 1. All coefficients are based on the same constant reference area, that is the area of the respective ideal wing (strake area excluded). Wetted areas

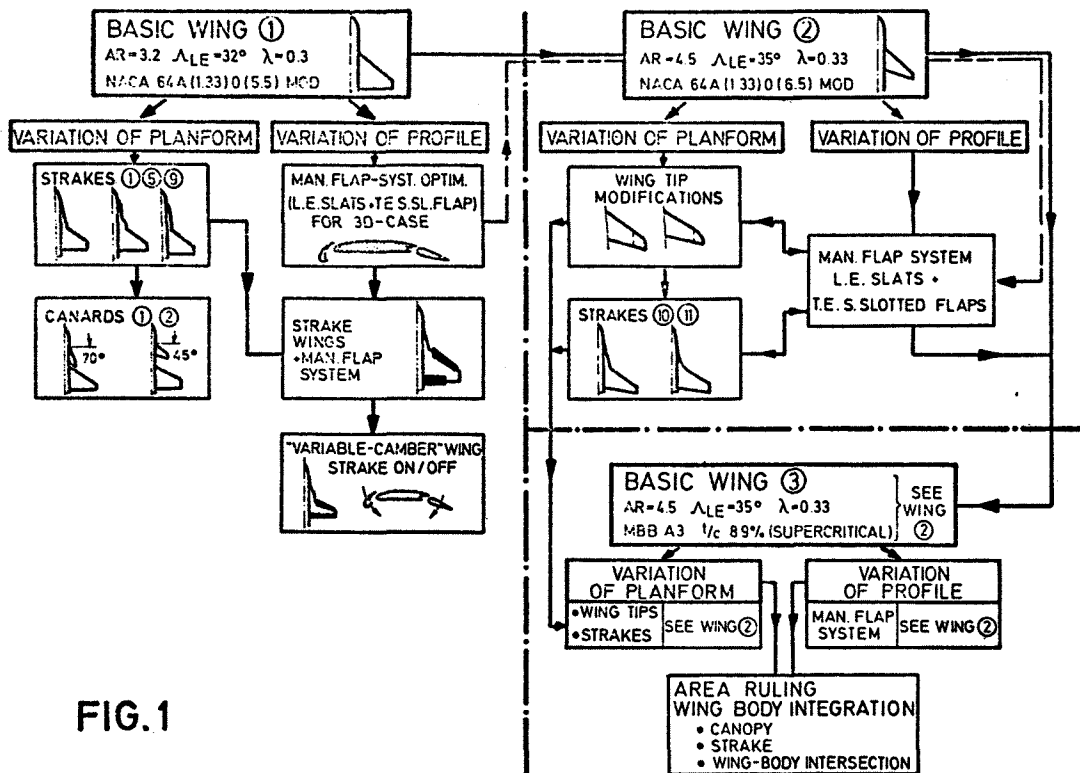


FIG. 1

EXPERIMENTAL 3-D APPROACH FOR IMPROVEMENT OF TRANSONIC PERFORMANCES

of all strakes are identical (10% of reference area). Test Reynolds-numbers were between 1.5 and 2.5 millions (based on the m.a.c. of the basic wings).

III. 1 Basic Wing ①

The trapezoidal planform ① was chosen from the following reasons:

- flap effectiveness
- weight
- stability (pitch-up due to the strake)
- buffet characteristics

III. 1.1 Strakes

As mentioned before, the strake is a device to generate controlled separation. Means of control of separation are the strake planform itself (sweep, slenderness) and section characteristics as leading-edge radius, twist and camber (for instance L.E. devices on the strake). Those effects were investigated, too but we shall concentrate on the general effects here, comparing results with and without strake ①.

Fig. 2 is a photograph of the pilot model with strake ① and maneuver flaps on the basic wing.

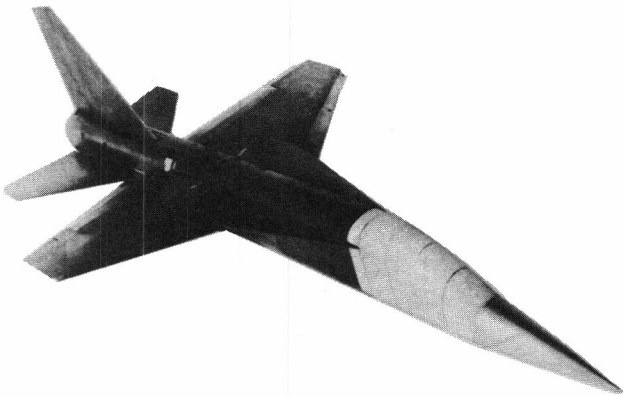


FIG. 2 PILOTMODEL WITH STRAKE 1

Fig. 3 gives the trimmed lift and drag data at $M = 0.8$ for the configuration with and without strake. Stability margin is 5%

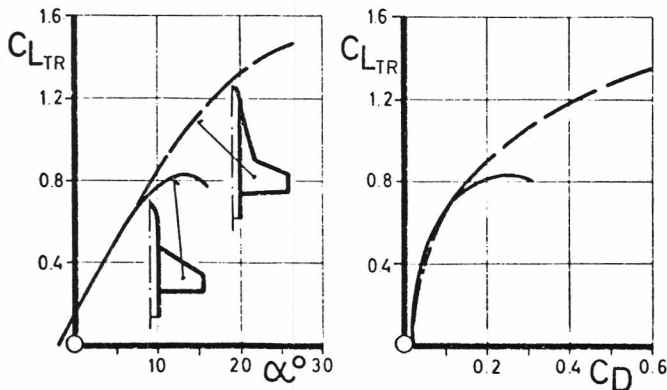


FIG. 3 EFFECT OF STRAKES ON TRIMMED LIFT AND DRAG CHARACTERISTICS
($M = 0.8$, 5% STABILITY MARGIN)

and is constant for both. Maximum trimmed lift is increased by the strake for more than 70% and an essential reduction of drag is found for high angles of attack. For low incidences the drag level of the strake wing is slightly higher than for the basic wing. This is originating in the effect of reducing the aspect ratio of the wing and a lift reduction induced by the strake on the basic wing. This is hidden for the lift data of the strake wing, as the strake area is excluded of the reference area.

Other important characteristics of the strake are plotted in Fig. 4.

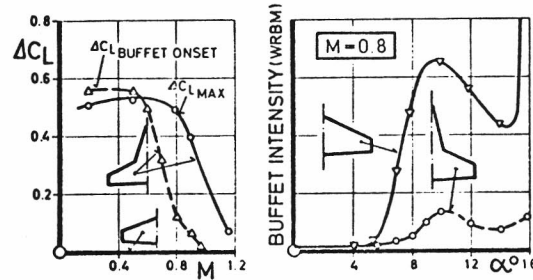


FIG. 4 IMPROVEMENT OF MANOEUVRE BOUNDARIES DUE TO STRAKE
(WING-BODY, CLEAN)

The left hand side of the graph demonstrates the increments of lift caused by the presence of the strake. A drastic increase of maximum lift is found all over the M -numbers shown (solid line). The same holds true for the buffet-onset lift (dotted line), if one takes into account, that this boundary (if it is any) is shifted to the left by $\Delta M = -0.2$. On the right hand side of fig. 4 the buffet intensity at $M = 0.8$ is drawn vs. a.o.a. For the strake configuration a mild divergence of the wing root bending moment oscillations was found at higher angles of attack, indicating a good buffet penetration. The question is, if buffet is any boundary for this configuration at all. Additionally the strake gives a 4% increase of drag divergence M -number and reduces the supercritical wave drag and trim drag. By the way the supersonic lift/drag ratio is improved considerably (20% at $M = 1.6$, $C_L \approx 0.4$). The reduction of trim drag is caused by the smaller supersonic neutral point shift of the strake configuration.

III. 1.2 Canards

The high lift production of the short coupled canards was generally inferior to the effect of the strakes of same exposed area. No data are shown here. A slight improvement relative to the strake data was found for lift/drag ratios in combination with the maneuver or high lift wing, as slats are then applied to the inboard part of the basic wing, too. But there are spoiling effects for the lateral/directional characteristics, imposed by the adverse side-wash gradients caused by the

high positioned canards. There is a considerable amount of trim power $C_{m\delta}$ due to the deflectable canards, but the canard induced total lift power $C_{L\delta}$ is zero for a large spectrum of angles of attack and canard incidences δ .

III. 1.3 Maneuver flap system

As mentioned before one of the reasons for the choice of planform ① was the relative high efficiency of maneuver devices on a thin wing like that. As all strake configurations were found to have lowest values of buffet onset lift at $M = 0.8$, it was decided to optimize a maneuver system in respect of the highest possible buffet free lift at this specific M-number. Maximum flap deflection should not exceed 8° for the sake of trimmed lift/drag ratios (hence depending on a given stability margin).

Fig. 5 is a typical graph taken out of this procedure finding an optimum slot position for a given angle of deflection and constant trailing edge flap setting. The

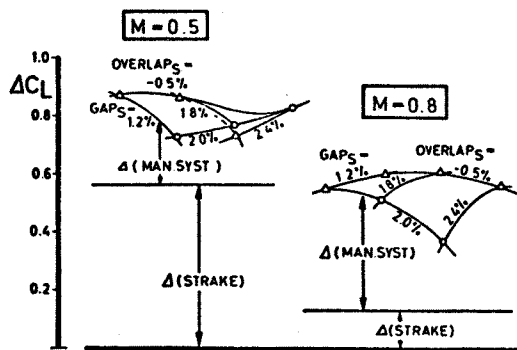


FIG. 5 EFFECT OF SLOT GEOMETRY OF LEADING EDGE SLAT ON BUFFET ONSET (CONSTANT: $\delta_S = -8^\circ$ $\delta_F = 8^\circ$ $O'LAP_F = 3\%$ $GAP_F = 2\%$)

trend for underlap is clearly to see (underlap: the slat trailing edge is in front of the basic wing section). Whilst the ratio of improvement

$$\Delta C_{L\text{Strake}} : \Delta C_{L\text{Man. syst.}} \text{ is closely to } 2:1$$

for subsonic cases, for transonic M-numbers this ratio is changing to approx. 1:4.

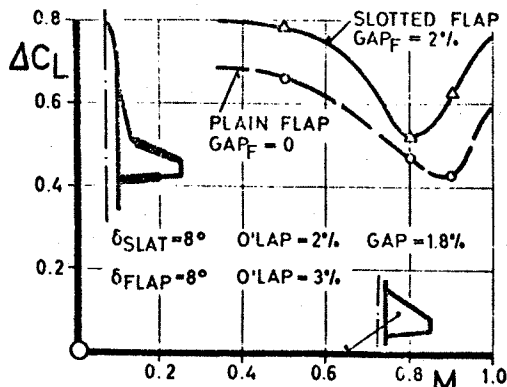


FIG. 6 EFFECT OF TRAILING EDGE FLAP SLOT ON LIFT BOUNDARIES (WING WITH STRAKE ① + L.E. DEVICES)

Fig. 6 demonstrates the effect of the trailing edge flap slot on the lift increments. The slotted flap is always superior.

The total improvement in buffet onset lift relative to the clean wing without strake is depicted in Fig. 7. The lower

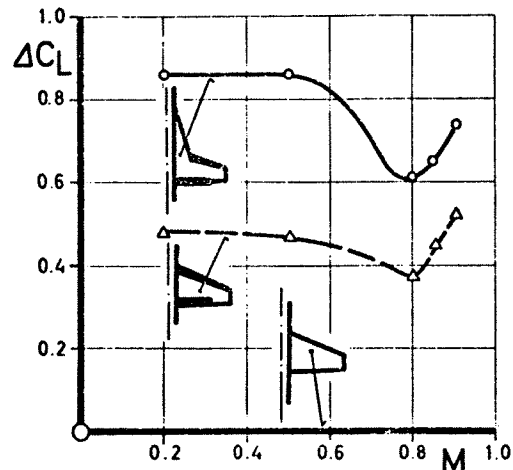


FIG. 7 IMPROVEMENT OF BUFFET ONSET LIFT DUE TO MANOEUVRE DEVICES FOR OPTIMUM FLAP SETTING

dotted line is representing the net effect of the optimized maneuver system on the basic wing (non identical with the data of fig. 6). The upper solid line compares with fig. 6, now giving the sum of improvements due to the strake plus the fixed maneuver system which is now optimized in presence of the strake. Hence the difference between the two curves in figure 7 is the net effect of the strake on the maneuver-wing. Compared to figure 4 (left) the effectiveness of the strake is reduced on the maneuver wing for subsonic cases. This is a tendency found for other characteristics, too.

A fixed maneuver system may be dictated by reasons of simplicity, structural considerations, limited tail power or trim drag aspects, the latter involving directly performance characteristics, especially for longitudinally stable configurations. Employing the CCV-technique of relaxed longitudinal stability the use of a "variable camber" wing is favoured. The deflection of the maneuver devices is then a function of angle of attack (better: load factor) and Mach number. One could speak of "chord wise variable geometry". The flap system takes over trim functions now. In this way the possibility arises to fly along the optimum polar (envelope of all maneuver polars).

Fig. 8 demonstrates this idea for two additional flap settings and a subsonic and transonic Mach number. Intermediate and extreme flap settings were left off for clarity reasons.

Fig. 9 gives an impression of the correlated angle of attack limit as a function of flap setting δ_F and Mach number. Dif-

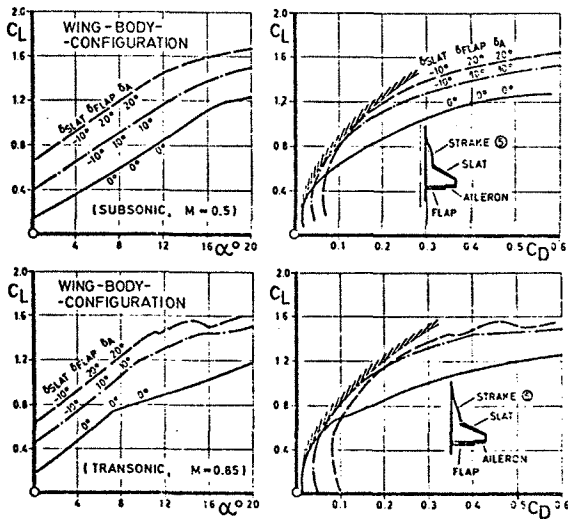


FIG. 8 "VARIABLE CAMBER"-WING: LIFT AND DRAG CHARACTERISTICS

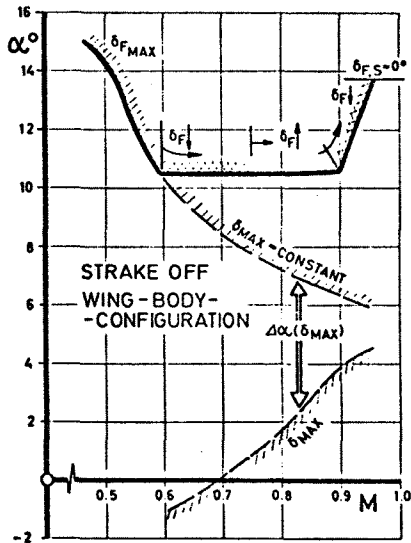


FIG. 9 "VARIABLE CAMBER"-WING: BUFFET-FREE ANGLE OF ATTACK REGIME

ferent regions $\alpha(M)$ were found to have different optimum deflections, the trends of which are symbolized by the corresponding arrows on δ_F . For demonstration purpose the lines of maximum flap angle δ_{max} are drawn in completely (dotted lines). A second lower angle of attack boundary was found for this case. Below this limit buffet phenomena were detected again thus drastically reducing the flight regime for this (far-off optimum) configuration.

The maximum incremental improvement of the buffet onset lift by the variable camber system is plotted in Fig. 10. The tendency shown here should also be true for limits as "moderate" and "heavy", because there is a strong divergence of oscillatory wing root bending moments for all configurations when a certain angle of attack or deflection is exceeded.

For $M \leq 0.85$ the system is more efficient for the wing without strake (upper bounda-

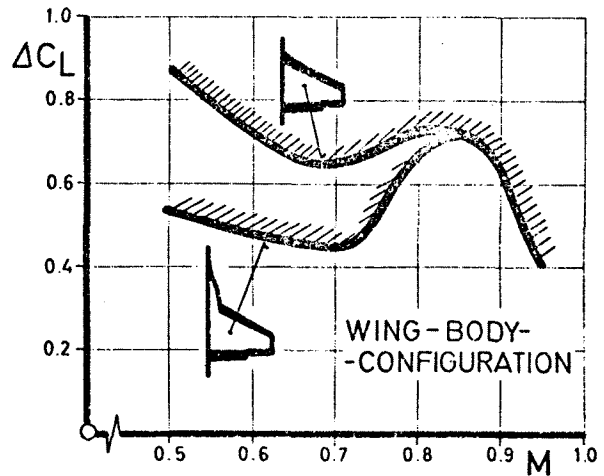


FIG. 10 IMPROVEMENT OF MANOEUVRE-BOUNDARY BUFFET-ONSET BY VARIABLE CAMBER SYSTEM FOR BASIC WING AND STRAKE WING

ry) but as the data are based on the respective unflapped wings the total boundary is better for the strake wing for all Mach numbers (the increment of the strake itself should be added from figure 4, to get the same basis, namely clean wing ① without strake).

III. 2 Basic Wing ②

Basic wing ② ($AR = 4.5$, $\lambda = 0.33$, $l_{LE} = 35^\circ$, wing section NACA 64A (1.33) 06.5 mod.) came out to be one corner point of a former parametric study. The choice of this planform was the easier as experimental data of almost an identical wing equipped with an early "peaky" supercritical airfoil were available (independent of the section MBB A3, later applied to basic wing ③).

III. 2.1 Variation of Planform

The wing planform was modified by replacing the conventional wing tip by a rounded "Bagley-type" one. Further variations consisted of two different strakes (strake ⑩ is the counterpart to strake ① with a straight 75° swept leading edge, strake ⑪ has a rounded leading edge, so that there is no leading edge break for this wing). The dominant effect of the rounded wing tips is a slight improvement of transonic performances, as shown in Fig. 11 for the buffet onset lift. This effect is more pronounced for the strake wing. The small negative increment (constant for $M \leq 0.5$) can be attributed directly to the loss of exposed area. The specific effects of different strake planforms (①, ⑤, ⑨) were, as they are all slender enough, of second order compared to their total effects for basic wing ① (regarding only longitudinal performances here). Lateral/directional characteristics are more strongly influenced by the shape of strakes. In contrast to that a comparison of the lift characteristics for strake wings ⑩ and ⑪ demonstrates remarkable differences at a subsonic and a tran-

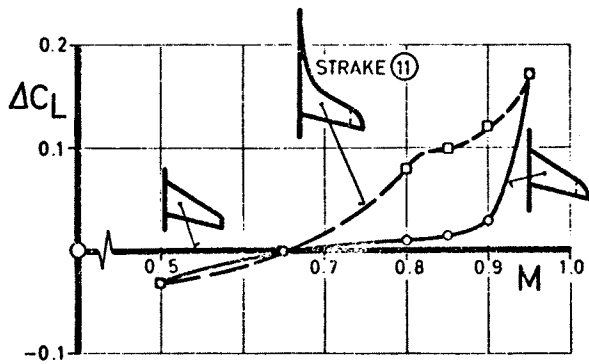


FIG. 11 EFFECT OF "BAGLEY-TYPE" WING TIPS ON BUFFET-ONSET LIFT FOR STRAKE AND BASIC WING
(BASIC WING ②, WING-BODY CONFIGURATION)

sonic M-number, attributed to the respective strake planforms. For subsonic Mach numbers the wing with strake ⑩ (straight L.E.) exhibits more lift at high angles of attack ($\alpha > 17^\circ$), whilst strake ⑪ is superior for a medium range $10^\circ < \alpha < 17^\circ$. The chordwise position of the vortex system of strake ⑪ is always closer to the leading edge, thus inducing more lift on the basic wing. But the vortex starts to burst earlier ($\alpha \approx 17^\circ$) over the wing. For transonic M-numbers (Fig. 12 right) there is an overall superiority of the configuration with strake ⑪.

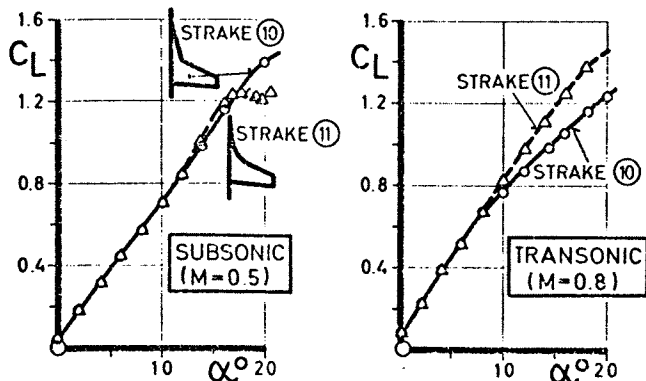


FIG. 12 EFFECT OF STRAKE PLANFORMS ON SUBSONIC AND TRANSONIC LIFT CHARACTERISTICS
(BASIC WING ②, WING-BODY CONFIGURATION)

The lift produced by strake-wing ⑩ breaks near an angle of attack $\sim \alpha = 8^\circ$. Strake ⑪ exhibits the more favourable shock formations due to the further outboard intersection of its leading edge with the basic wing (41.5% instead of 29.5% semispan). Thus the a.o.a. for shock induced separations is shifted to higher incidences. This is directly reflecting on the lift and drag characteristics of the configurations.

III. 2.2 Maneuver flap system

The maneuver flap system of basic wing ① was scaled for the 1% thicker section of

basic wing ② and was positioned then in the same locations as before (full span slat: $\delta_s = -8^\circ$, $o'laps = -0.5\%$, $gap_s = 1.8\%$ / single slotted flap: $\delta_f = 8^\circ$, $o'lap_f = 3\%$, $gap_f = 2\%$). The general effects of the maneuver system are found to be in analogy with the results obtained with wing ① (see II. 1.3) and need not to be repeated again. The tendency of reduced effectiveness of the maneuver flaps in combination with the strake wing is still more pronounced for basic wing ②. This is demonstrated in Fig. 13 for the increments of buffet onset lift caused by the maneuver devices and maneuver devices plus strake ⑪ relative to the clean basic wing ②.

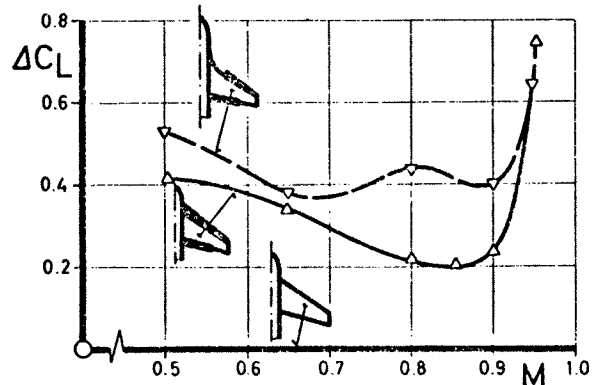


FIG. 13 IMPROVEMENT OF BUFFET CHARACTERISTICS DUE TO MANOEUVRE FLAPS AND STRAKE
(BASIC WING ②, WING-BODY CONFIGURATION)

This figure compares directly with figure 7 (respective increments for basic wing ①). In addition the maneuver flap system is less effective for the swept wing configuration ②.

III. 3 Basic Wing ③

Basic wing ③ differs from wing ② only by the invention of the supercritical section MBB A3 (rel. thickness $t/c = 8.9\%$ streamwise). The wing was modified by the same variations already applied to wing ② such as strakes, wing tips and a maneuver flap system. We shall concentrate on the effects of the supercritical profile referred to the clean and maneuver configuration.

III. 3.1 Development of Supercritical Wing Section

A hodograph method based on Sobieczky's theory of rheoanalog has proven to be a helpful tool in finding shockless transonic airfoils.

The airfoil contour is represented by the boundary velocity diagram (Fig. 14) specified by the designer, and serves as input. The procedure of mapping the section into the physical plane is achieved then by several successive steps. The boundary is distorted by a special conformal mapping into a cylinder, which is immersed in

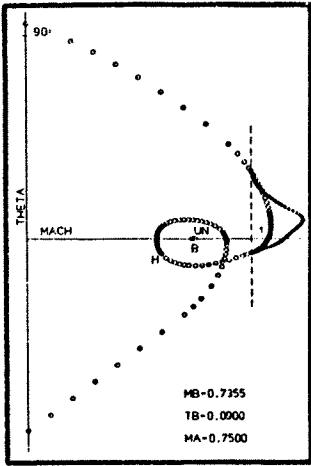


FIG. 14

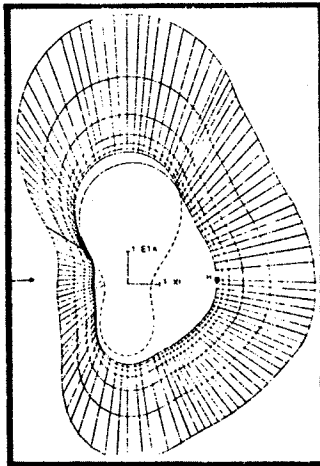


FIG. 15

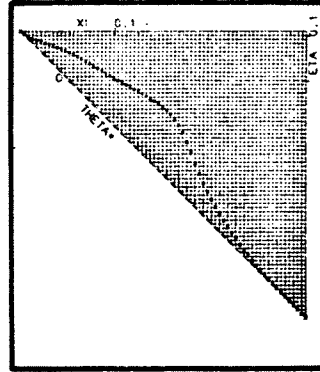


FIG. 16

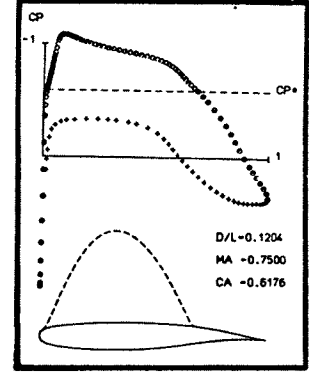


FIG. 17

FIGURES 14 + 17 SUPERCRITICAL SECTION: DESIGN-PROCESS

a uniform onset flow of known free stream direction (Fig. 15). In this elliptical working plane the potential along the subsonic boundary is computed by a constant strength panel method allowing for the correct representation of the compressibility in the flow field. The values of the stream- and potential functions along the sonic line are transferred to the characteristic plane (Fig. 16). An initial boundary value problem is solved then leading directly to a new supersonic boundary (different from that specified by the input) and the respective potential distribution.

Since boundary velocity vectors and potential distribution are known, the airfoil coordinates and the according pressure distribution can be obtained in the physical plane by integration (Fig. 17).

A family of supercritical wing sections was then tested at ARA-Bedford in the 18 x 8 inch transonic profile tunnel. Section MBB A3 was selected for application on basic wing ③ (Fig. 18).

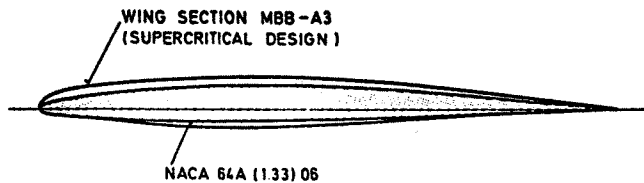


FIG. 18 COMPARISON OF WING SECTIONS

The decision for this (relatively conservative) section was strongly influenced by analysing the off-design behaviour and trim aspects, especially important for a fighter-type aircraft. The section is characterized by a small amount of rear loading and a roof top extension to 50% of the chord. It was designed for a lift coefficient $C_L = 0.5$ at $M = 0.75$.

This compares with an experimentally found design point $C_L = 0.52$ at $M = 0.76$.

III. 3.2 Supercritical Wing Results

The section was applied to wing ③ strictly applying identical rules for camber and twist distribution. Hence the only parameter changed in comparison to wing ② is the profile.

Transferring the 2-d data on to the wing-body configuration gives a theoretical design point for wing ③ defined by $C_L = 0.36$, $M = 0.842$, the experimental verification of which is demonstrated in Fig. 19

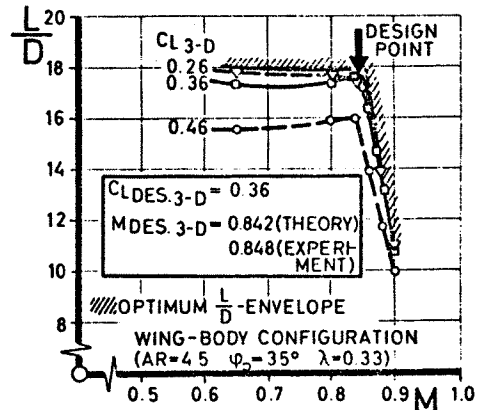


FIG. 19 SUPERCRITICAL DESIGN: VERIFICATION OF THEORETICAL DESIGN POINT BY EXPERIMENT

For different lift coefficients the lift/drag ratio is plotted vs. M-number. Optimum L/D envelope is drawn for comparison. The experimentally found design point came out to be in good agreement with the theoretically predicted one, differing slightly in the design M-number ($M = 0.848 \rightarrow 0.842$).

As mentioned before the off-design characteristics of the section were carefully watched from the beginning. There were in mind bad experiences earlier learned with

a "peaky" type profile, exhibiting separation effects near the leading edge for subcritical cases.

Fig. 20 gives the results of the design and off-design characteristics of wing ③ compared to the conventional wing ② (dotted line).

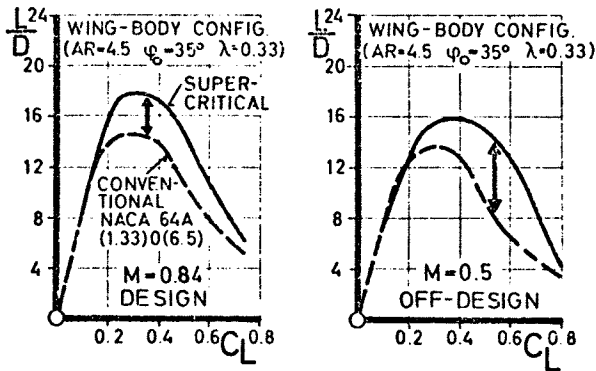


FIG. 20 SUPERCRITICAL DESIGN: COMPARISON DESIGN / OFF-DESIGN RESULTS

For example there are gains for wing ③ of nearly 100% in lift/drag ratio at $C_L = 0.6$ and $M = 0.5$. This may be directly attributed to the avoidance of leading edge separation by the blunt nose of the air-foil.

Fig. 21 was plotted to give a survey of the relative merits of the two designs.

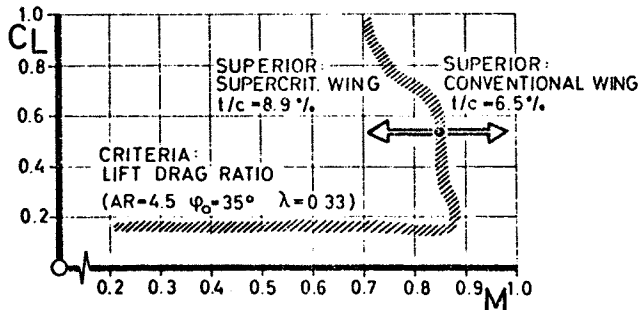


FIG. 21 SUPERIORITY OF WING-DESIGNS

Lift coefficients corresponding to the intersections of the different lift/drag ratio curves (as shown in figure 20) were drawn as a function of M-number. In this way a boundary is found which divides the field C_L (M) in regions of relative superiority. As the intersections are rather smooth, the borderline is represented by the dashed band. It is easy to see that the superiority of the supercritical design is terminated rather by exceeding its design M-number than by excursion over its design lift coefficient $C_L = 0.36$.

Pressure distribution data of the exposed wing are plotted in Fig. 22 for $M = 0.85$ and an angle of attack $\alpha = 1^\circ$, giving a total $C_L = 0.36$.

The inboard sections are strongly influenced by the presence of the body. The pressure distribution at the mid board

$M = 0.85$
 $\alpha = 1^\circ$

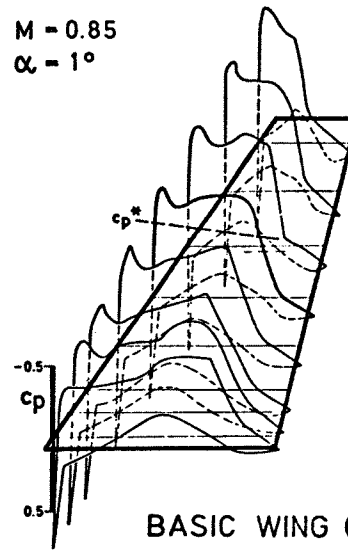
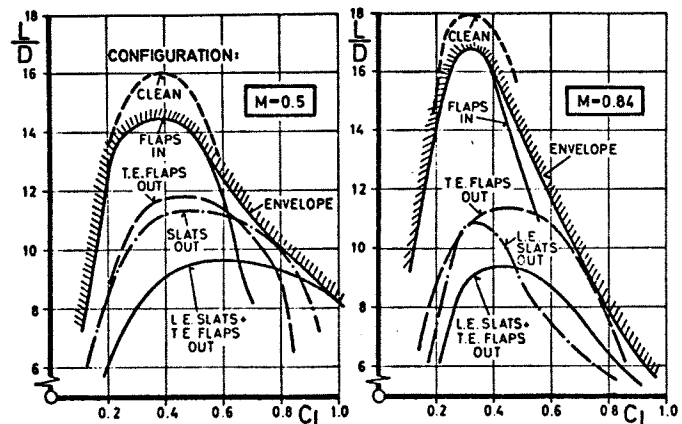


FIG. 22 BASIC WING ③

section (fat line) is in fair agreement with the 2-d design data. The amount of supercritical flow is demonstrated by the intersection with the line of critical pressure c_p^* . There is an indication for the rise of the initial tip shock, but separation effects could not be found anywhere.

III. 3.3 Maneuver Flap System

The maneuver devices were designed in the same way as described for wing ② (see III. 2.2). Slat and flap positions and deflections are identical. No further attempt was made to optimize the system for wing ③. The separate and combined effects of flaps and for slats are plotted in Fig. 23 for a subsonic and transonic M-number. Generally the flapped wing exhibits a reduction of max. L/D even in the flap-in configuration when compared to the data of the clean wing. For the subsonic case ($M = 0.5$) slats are more effective in expanding the envelope than the T.E. flaps (for these fixed deflections $\delta_s = -8^\circ / \delta_f = 8^\circ$). The opposite is true for the transonic case ($M = 0.84$). These characte-



EFFECT OF MANOEUVRE DEVICES ON LIFT/ DRAG RATIO FOR SUBSONIC AND TRANSONIC MACH-NUMBERS (BASIC WING ③(SUPERCritical SECTION), WING-BODY CONFIGURATION)

istics stem from the different sources causing separation at those specific Mach numbers. Subsonic separation and increase of drag start at higher angles of attack, hence favouring the slat effect to shift maximum lift to higher incidences restoring the flow around the leading edge. On the other hand the shock induced separations at transonic M-numbers start at lower angle of attack and are favourably shifted to higher C_L -values when the slotted T.E. flap is deflected. It is emphasized again that for other combinations of slat/flap deflections than those used here, the characteristics may change.

Fig. 24 gives the increase of usable lift due to the devices, as defined by the shift of the break in the lift curve slope for stall approach.

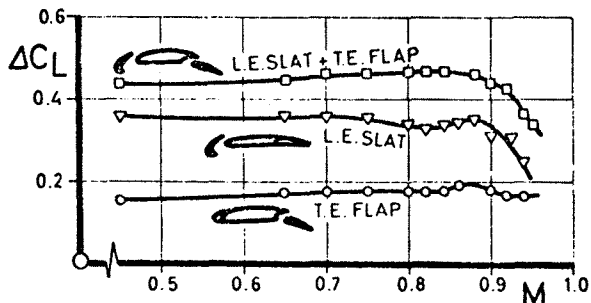


FIG. 24 EFFECT OF MANOEUVER DEVICES ON LIFT BOUNDARY OF BASIC WING ③ (WING-BODY CONFIGURATION)

For this high angle of attack boundary the slat is clearly superior, giving about twice the increment produced by the flap for $M < 0.8$.

III. 3.4 Wing-Body Integration

Finally an attempt was made to integrate the wing-body configuration by adding volume to the strake, to the fuselage and the forebody/canopy in the wing-body intersection region. Removing mass from the original body was forbidden because of reproducibility of the original fuselage. The effort was to find a compromise in straightening the wing isobars in proximity of the body and smoothing kinks in the cross-sectional area distribution. In comparison with the magnitude of improvement found by the invention of strakes, maneuver flap systems or the supercritical airfoil, the respective increments due to this attempt were of minor order. For instance an increase of drag-divergence M-number of 0.012 was realized. The effect of the wing-body integration on the lift boundary C_{L_B} (as defined by the first break in $C_L(\alpha)$) is shown in Fig. 25 together with the results of clean wing ② and the unmodified wing ③.

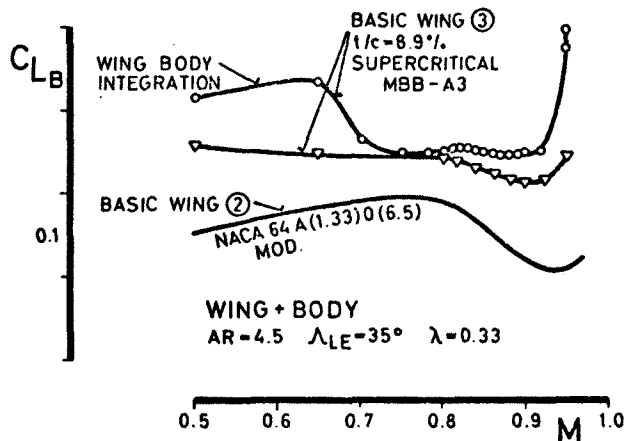


FIG. 25 EFFECT OF WING-BODY INTEGRATION ON LIFT BOUNDARY C_{L_B} (AS DEFINED BY 1st BREAK IN $C_L(\alpha)$)

Lift/drag data are plotted in Fig. 26 for a M-number of $M = 0.84$. The effect of wing-body integration is compared with the results obtained by the combination of wing ③ with the unmodified strake ①, which then does not have a blunt leading edge (dotted line). So the superiority of the "integrated" configuration for low α ($C_L < 0.53$) is attributed to the suppression of the strake vortex system as a consequence of the blunt nose section, whilst for increased angles of attack the configuration with the sharp strake withdraws profits from the strake as a "non linear" working device.

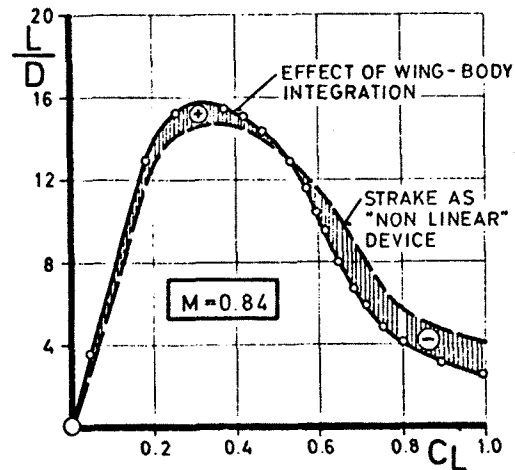


FIG. 26 EFFECT OF WING-BODY INTEGRATION ON LIFT/DRAG RATIO (BASIC WING ③ + STRAKE ①)

IV. REFERENCES

- Sacher, P. / Pfanzeder, D.
Nichtlineare Theorie schlanker Flügel
Teil 1: Voruntersuchungen im Wasserkanal
EWR Ber. 459-69 1969
- Sobieczky, H.
Analog-analytische Konstruktion überkritischer Profilumströmungen
DGLR 72-129 1972
- Staudacher, W.
Verbesserung der Manöverleistungen im hohen Unterschall
MBB-UFE896-72(Ö) / DGLR 72-126 1972
- Eberle, A.
Entwurf transsonischer Profile nach dem Limitline-Kriterium
MBB-UFE899-72(Ö) 1972
- Zech, A. / Staudacher, W.
Transsonische Profil- und Flügelformen: Hochauftriebsmittel für den Luftkampf
MBB-UFE908-72 1972
- Eberle, A. / Sacher, P.
Tragflügelentwurf für transsonische Strömungen
MBB-UFE1058 1973
- Bretthauer, N. / Sacher, P. / Staudacher, W.
Flügel-Rumpf-Integration
MBB-UFE910-72 1972
- Zech, A. / Staudacher, W. / Bretthauer, N.
Untersuchungen im Unterschall an Flügeln mit Strakes für Kampfflugzeuge
MBB-UFE1019 1973
- Staudacher, W.
Flügel mit Strakes (experimentell)
MBB-UFE1059 1973
- Staudacher, W.
Zum Einfluß von Flügelgrundriß-Modifikationen auf die aerodynamischen Leistungen von Kampfflugzeugen
MBB-UFE1033(Ö) / DGLR 73-71 1973
- Staudacher, W.
Flügel mit Strakes (experimentell)
MBB-UFE1154 1974
- Eberle, A.
Experimentelle Untersuchungen überkritischer Profile und Tragflügel im Hochgeschwindigkeitsbereich
MBB-UFE1153 1974
- Krahl, H.
Untersuchungen der Interferenz und Lastverteilung bei Kampfflug-Konfigurationen mit Strakes
VFW-F 4.01/74 1975
- Eberle, A.
Eine exakte Hodographenmethode zum Entwurf überkritischer Profile
MBB-UFE1168(Ö) 1975
- Baumert, W.
Messungen am Prinzipmodell Flügel mit Strake bei symmetrischer Anblasung
DFVLR i.B. 157-75 A13 1975
- Baumert, W.
Druckverteilungsmessungen am Prinzipmodell Flügel mit Strakes bei unsymmetrischer Anblasung
DFVLR i.B. 157-75 A17 1975
- Eberle, A.
Transsonischer Tragflügel: Theoretische und experimentelle Untersuchungen zum Flügel/Rumpf-Entwurf
MBB-UFE1222 1976
- Staudacher, W.
Flügel mit Strakes
MBB-Report in preparation